Computers and Concrete, *Vol. 25, No. 1* (*2020*) *67-73*
DOI: https://doi.org/10.12989/cac.2020.25.1.067

Computer aided failure prediction of reinforced concrete beam

A.B.M. Saiful Islam*

Department of Civil & Construction Engineering, Imam Abdulrahman Bin Faisal University, 31451, Dammam, Saudi Arabia

(*Received May 17, 2019, Revised December 25, 2019, Accepted January 10, 2020*)

Abstract. Traditionally used analytical approach to predict the fatigue failure of reinforced concrete (RC) structure is generally conservative and has certain limitations. The nonlinear finite element method (FEM) offers less expensive solution for fatigue analysis with sufficient accuracy. However, the conventional implicit dynamic analysis is very expensive for high level computation. Whereas, an explicit dynamic analysis approach offers a computationally operative modelling to predict true responses of a structural element under periodic loading and might be perfectly matched to accomplish long life fatigue computations. Hence, this study simulates the fatigue behaviour of RC beams with finite element (FE) assemblage presenting a simplified explicit dynamic numerical solution to show computer aided fatigue behaviour of RC beam. A commercial FEM package, ABAQUS has been chosen for this complex modelling. The concrete has been modelled as a 8-node solid element providing competent compression hardening and tension stiffening. The steel reinforcements are simulated as two-node truss elements comprising elasto-plastic stress-strain behaviour. All the possible nonlinearities are duly incorporated. Time domain analysis has been adopted through an automatic Newmark-β time incremental technique. The program consists of twelve RC beams to visualize the real behaviour during fatigue process and to obtain the reliability of the study. Both the numerical and experimental results indicate a redistribution of stresses along the time and damage accumulation of beam which severely affect the serviceability and ultimate capacity of RC beam. The output of the FEM analysis demonstrates good match with the experimental consequences which affirm the efficacy of the computer aided model. The controlled fatigue damage evolution at service fatigue load limits makes the FE model an efficient tool in predicting high cycle fatigue behaviour of RC structures.

Keywords: computer aided modelling; failure prediction; fatigue; cyclic loading; explicit dynamic; cracks; damage; reinforced concrete beam

1. Introduction

Structural members experience fatigue failure because of repeated or cyclic stresses which alters the essential characteristics of constituent materials. While failure, the load is generally lower than tensile or yield strength of material under static load. Its three distinct phases are crack initiation in the stress concentration regions, incremental crack propagation and final catastrophic failure. As the failure is brittle, sudden and catastrophic; people are becoming much concern about this failure especially for the public structure like bridge, flyover etc. Usually, these structures suffer heavy traffic loading cycle which eventually generate repetitive tensile stresses.

The fatigue process in concrete reforms the internal structure in a progressive manner which result in the gradual progression of internal micro cracks and finally advance with irrecoverable strain. A number of academics have investigated the fatigue performance of normal concrete ACI (1992), lightweight concrete (Sohel *et al*. 2018), FRP composites (Sarkani *et al*. 2001), steel reinforcement (Helagson and Hanson 1974, Moss 1982) and reinforce concrete structure (Sasaki *et al*. 2010) separately. Concrete fails at stress below its ultimate static strength when cyclically loaded to failure and exhibit strain softening behavior (Huda *et al*. 2017, Rahman *et al*. 2017). Several factors may influence the fatigue performance of RC element like loading condition and frequency, stress level, boundary conditions, number of cycles, matrix composition, stress ratio etc. Precise fatigue experimental test considering all the factors in laboratory is extremely costly due to the prolong test duration and associated establishment overheads. It is too difficult to conduct tests under such constrained conditions. Whereas, the numerical simulation technique doesn't have any limit to its application (Islam *et al*. 2014, Islam *et al*. 2015, Maekawa *et al*. 2003, Suidan and Schnobrich 1973). A few researchers performed nonlinear finite element analysis to predict RC beam behavior under monotonic loading (Barros *et al*. 2013, Hawileh 2012, Zhang and Teng 2014).

However, the challenges of modelling nonlinear response include: concrete compression and tension damage behavior, tension stiffening behavior of steel and strengthening material, characterizing bond-slip relationship amid reinforcing steel and concrete (Omran and El-Hacha 2012). Though very few studies attempted to resolve these issues under monotonic loading, the nonlinear finite element analysis is scarce for dynamic or fatigue loading. The computational process to simulate the fatigue life studies habitually involves the structural responses under a small fraction of real loading and then might be extrapolated over many load cycles to predict the crack

*Corresponding author, Ph.D.
E-mail: asislam@iau.edu.sa

http://www.techno-press.org/?journal=cac&subpage=8
ISSN: 1598-8198 (Print), 1598-818X (Online)

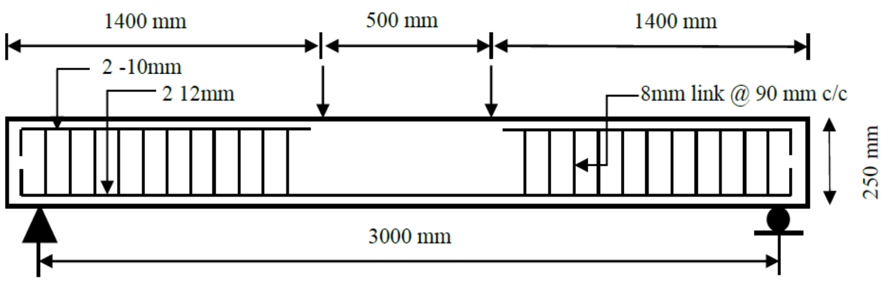

Fig. 1 Specimen details

Table 1 Matrix of selected RC Beam specimens

Beam ID	Specimens for fatigue analysis	
	Min-Max[a] (%)	Range of loading (%)
F1	10-35	25
F2	10-40	30
F3	10-45	35
F4	10-50	40
F5	10-55	45
F6	10-60	50
F7	10-65	55
F8	10-70	60
F9	10-75	65
F10	10-80	70
F11	10-85	75
F12	10-90	80

initiation and propagation (Aslani and Jowkarmeimandi 2012). Al-Rousan and Issa (Al-Rousan and Issa 2011) conducted FEM analysis on strengthened RC beam under fatigue loading where the fatigue stress range of 0.45 f_y-0.90 f_y showed significant impact on the tested samples.

Conventional Implicit dynamic analysis is very expensive for high level computation. The dynamic analysis in ABAQUS/Explicit offers a computationally potential modelling approach to get factual responses of a structural element under periodic loading and is found to be matched to achieve long life fatigue calculations. Hence, the purpose of the study is to simulate the fatigue behavior of RC beams with finite element (FE) assemblage presenting a simplified numerical solution. The study investigates the influence of loading range on the ultimate load capacity, deformation and failure mode of RC beams under fatigue loading.

2. Materials and methods

2.1 Specimens configuration

A total of twelve RC beam specimens have been selected in the study for fatigue analysis. Loading ranges and the loading frequencies are varied in the modelled beam under fatigue. All the beam specimens have been simulated in FE package and has been investigated under fatigue case. The matrices of the beam specimens have been shown in Table 1.

The specimens have been designed in under reinforced condition using 0.85% steel to get flexural failure as per the ACI code [23]. The 3300 mm long rectangular beam has cross-sectional dimension of 125 mm×250 mm with an effective span of 3000 mm and 1250 mm shear span. Two 12 mm diameter deformed steel bars are used as tension reinforcement. These are bent in ninety degrees at both ends to fulfil the anchorage criteria. On top compression area, two 10 mm diameter deformed steel bars have been fabricated as hanger bar merely in the shear span zone. The shear reinforcement comprises 8 mm diameter plain steel bars spaced at 90 mm interval. Fig. 1 shows the detail beam configuration.

The beams are prepared using ready mix concrete. Graded crushed granite stone is used as coarse aggregate and natural sand as fine aggregate. The 28 days compressive strength and flexural strength of hardened concrete are 59 MPa and 5.5 MPa respectively based on the cube (100 mm×100 mm×100 mm), and prism specimens (500 mm×100 mm×100 mm), respectively as per ((ASTM, 2014, BS EN 2009, BS EN 2009) BS EN 2009), and (BS EN 2009). The ASTM A615 (A615M-14 2014) specification has been followed to check the mechanical properties of deformed steel bars. The yield stress and elastic modulus are 520 MPa and 200 GPa respectively. However, the shear reinforcement has yield stress of 380 MPa maintaining elastic modulus alike deformed bars.

2.2 Numerical simulation

The numerical study comprises steel reinforcement and concrete. Consistent constitutive models relevant to reinforcement and concrete are simulated in the ABAQUS environment (Hu *et al.* 2004). The selected considerations of material characteristic as well as the constitutive models are deliberated subsequently.

2.2.1 Steel reinforcement

The steel reinforcement modulus of elasticity used in the analyses E_S=200 GPa. The steel reinforcement stress-strain curve is considered as elasto-plastic as shown in Fig. 2. The reinforcement is considered as an equivalent uniaxial material all over the element section. Between concrete and steel, perfect bonding is assumed. The appropriate model of constitutive behavior of the reinforcement along with its cross-sectional area, position, spacing and orientation of each layer of reinforcement in each element are specified.

2.2.2 Concrete

The compressive strain of concrete, ε_o at peak stress f'_c is

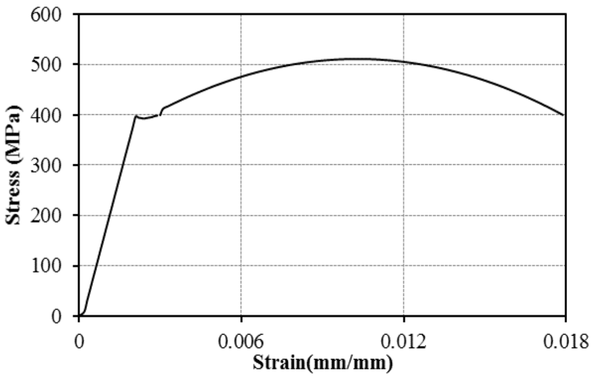

Fig. 2 Elasto-plastic model for reinforcement

chosen as 0.003 that falls in the ACI Committee 318 (Committee 2011) recommended demonstrative value 0.002-0.003 under uniaxial compression. The poison's ratio v is used as 0.20 which resembles to the appropriate range of 0.15-0.22 under uniaxial compressive stress (Nilson, 1982). The uniaxial tensile strength of concrete f_t' is taken (Hu *et al*. 2004) as

$$f_t' = 0.33\sqrt{f_c'} \quad \text{MPa} \tag{2}$$

The elastic modulus of concrete E_c is vastly correlated to its compressive strength as per the empirical formula (Committee 2011).

$$E_c = 4700\sqrt{f_c'} \quad \text{MPa} \tag{3}$$

Under multiple stress conditions, the maximum strength envelope is mainly independent of load path (Kupfer *et al.* 1969). A Mohr-Coulomb genre compression model with a crack detection surface is employed to model the concrete failure.

An elastic-plastic theory related to flow and an isotropic hardening principle is used in concrete modeling. When cracks occur in the detection surface, then damaged elasticity simulates the cracks (Hibbitt 2007). The effective stress (σ_c) and strain (ε_c) of concrete correlation (Desayi and Krishnan 1964) follows the accepted uniaxial stress-strain curve as in Eq. (4).

$$\sigma_c = \frac{E_c \varepsilon_c}{1 + (R + R_E - 2)\left(\frac{\varepsilon_c}{\varepsilon_0}\right) - (2R - 1)\left(\frac{\varepsilon_c}{\varepsilon_0}\right)^2 + R\left(\frac{\varepsilon_c}{\varepsilon_0}\right)^3} \tag{4}$$

$$R = \frac{R_E(R_\sigma - 1)}{(R_\varepsilon - 1)^2} - \frac{1}{R_\varepsilon}, R_E = \frac{E_c}{E_0}, E_0 = \frac{f_c'}{\varepsilon_0} \tag{5}$$

Here, R_σ=4 and R_ε=4 (Hu and Schnobrich 1989).

The micro crack behavior of concrete is represented by utilizing the smeared model. The reinforced concrete member cracked section still convey some tensile stress in the normal direction to the crack named as tension stiffening (Nilson 1982). In the model of concrete tension stiffening, throughout the post cracking phase, the cracked RC section carry-over shear forces through the interlocking of aggregate or shear friction calling as shear retention.

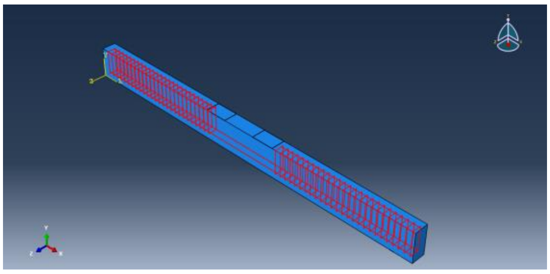

Fig. 3 3D non-linear finite element model of reinforcements

2.3 Commuter aided modelling

For modelling actual behavior of RC beams, the concrete volume has been simulated as 3D solid elements. These are in fact 8-node reduced integration solid hexahedron elements comprising three degrees of freedom at each node. The principal benefit of incorporating solid elements with single-point volume integration performed by Gaussian quadrature is the extensive savings in computer time nonetheless they suitably controls the zero energy modes. For resisting this undesirable hourglassing, three-dimensional algorithms for are considered.

The longitudinal steel bars and transverse ties are simulated using 2-node truss elements (Fig. 3). The truss elements have also three degrees of freedom at each node. The 8-node solid elements are 1086 in numbers consisting 1724 nodes. From the numerical convergence study, such mesh size has found to be optimum. There are 824 truss elements. The concrete element naming is C3D8R which considers reduced integration with hourglass control. In addition, for steel reinforcement, T3D2 employs linear interpolation for position and has a constant stress.

A huge number of small time increments have been used in the explicit dynamic analysis efficiently for the RC specimens. Each increment is rather cheap compared to the implicit dynamic analysis as there is no need for solving a set of simultaneous equations. The equations of dynamic equilibrium at the initial stage of increment, t is gratified by the explicit central-difference operator. The accelerations at time t have been utilized to advance the velocity solution to time $t+\Delta t/2$ as well as the displacement solution to time $t+\Delta t$. Apart from the fixed value, the time incrementation scheme has been used as fully automatic in this study which requires no user intervention.

During the loading, the self weight of the beams have been captured as gravitational force obtained from the mass of individual element. Distributed pressure forces are applied for the imposed loading. Initially, such pressure load is given as ramp up to computed upper level of load-control case. Then after the monotonic investigation is feed by displacement control loading. As with boundary conditions, loads applied use appropriate amplitude references. For fatigue investigation, cyclic loading with required amplitude has been imposed after an initial loading employed by a ramp.

2.4 Fatigue rationale

The stress limits recommended by the Canadian

Highway Bridge Design Code [10] stipulates a maximum stress range in the tension steel of 125 MPa. However, ACI Committee 440 [16] suggested that the peak stress should not exceed 80% of the yield stress. In the study, 35%, 40%, 45%, 50%, 55%, 60%, 65%, 70%, 75%, 80%, 85% and 90% of the beam ultimate capacity has been tested to observe the fatigue behavior within, below and beyond the serviceability limit condition. In most of the case 60% of the ultimate capacity is considered as the serviceability limit of a beam. The minimum load is chosen as 10% of the beam ultimate static capacity which is basically the dead load capacity of the structure. The sample is kept under load control mode until the yielding of internal steel; after that position control has been enabled up to the failure of beam.

For fatigue loading, an initial load of 10% ultimate capacity plus corresponding load amplitude has been imposed in ramp. Then for 2 million fatigue cycles the periodic loading is applied to determine the fatigue load limits which includes the fatigue cycling with damage accumulation, the energy dissipation, and the permanent deformation. The beams are loaded until the tension steel strain reaches to a desired percentage of ultimate capacity and then unloaded unto the strain experiences reaches a stress equivalent to 10 % of ultimate capacity. The loads at which the beams reaches the lower and upper strain values in the tension steel are considered as the maximum and minimum fatigue limits for the fatigue loading cycles in load control mode. Two million cycles have been applied to the beams at a frequency of 2 Hz with the computed amplitudes.

3. Results and discussions

3.1 Validation of computer aided model

The experimental beam published by Badawi and Soudki (2009) has been simulated in ABAQUS package considering similar specifications and the behavior has been compared. It reveals that together with the experimental study, the numerical approach is noticeably suitable tools to predict the structural behavior of RC elements.

Under cyclic loads for 10-75% load range of ultimate load 64 KN, the maximum beam deflections behaviors for numerical beam have been found in good agreement with a trivial difference of 2~7% with Badawi and Soudki (2009). Identical behavior for the same load range is found for both the selected experimental and numerical beams. The increase in the deflection with number of cycles is obvious. At large, stabilized deflection versus percentage of the fatigue life has been detected. The specimens show an upsurge in the deflection in the first 10% of their fatigue life, followed by a stable deflection before the failure stage. The closely matching values accomplished in the computer aided study confirm the validity of the numerical model.

3.2 Fatigue life analyses

The fatigue life of the representative beams is shown in Table 2. It has been observed that up to 45% upper load of ultimate loading, the RC beams do not fail even within 2 million cycles. It is desirable that beams subjected to lower load ranges shows longer fatigue lives compared to the beams under higher load range. At a load range of 15.6 kN (10~50% of ultimate capacity), the beam fails at 1.66716 million cycles, while for 23.4 KN (10~70% of ultimate capacity) the beam has a fatigue life of 0.604 million cycles. Thus, with increasing the upper load by 20%, the life decreases by around three times. The fatigue life endurance limit for the RC beams for different cases are discussed in the subsequent section.

Table 2 Fatigue life of the RC beam specimens

Beam ID	Upper load (%)	Load range (%)	Failure cycles (million)
F1	35	25	No failure
F2	40	30	No failure
F3	45	35	No failure
F4	50	40	1.66716
F5	55	45	1.3114
F6	60	50	1.2150
F7	65	55	0.8544
F8	70	60	0.604
F9	75	65	0.352
F10	80	70	0.286
F11	85	75	0.236
F12	90	80	0.152

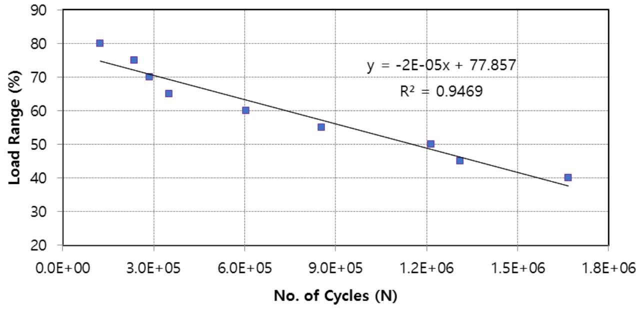

Fig. 4 S-N curve predicting fatigue behavior

3.3 S-N curve

From the study, an S-N curve has been introduced to understand the basic characteristics of the RC beam under fatigue. The S-N curve showing percentage of load range against number of cycles to failure have been demonstrated in Fig. 4. It is seen that the predicated line is a straight line with a good regression value. This is meaning that the failure results of different loading conditions are reasonable. A gradual decrease in fatigue life is seen from the S-N curve. The equation of the linear variation has been shown in the illustration. The developed S-N curve can be representative for prior prediction of the fatigue behavior in case of any loading condition for the selected RC beam prototype.

3.4 Behavior of RC beam under fatigue

3.4.1 Deflection behavior

Fig. 5 presents the load-deflection relation at mid span,

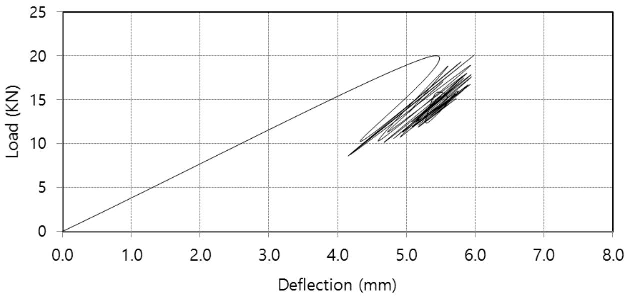

Fig. 5 Load versus deflection comparison

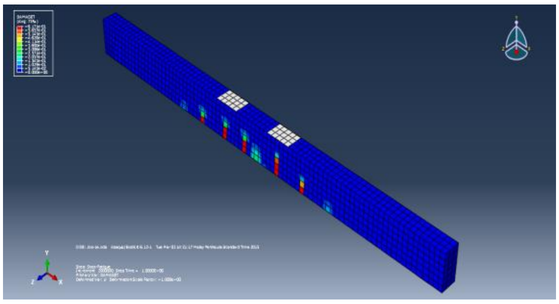
Fig. 6 Crack pattern

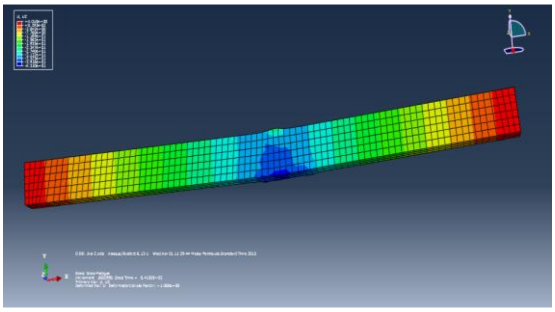
Fig. 7 Displacement at 1.66716 million cycles

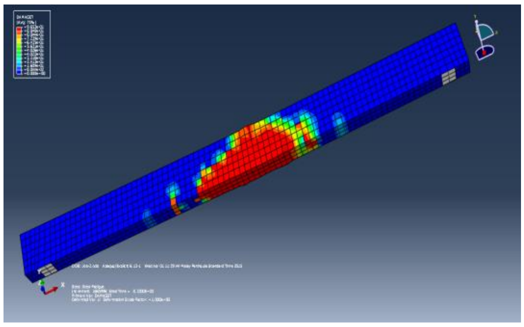
Fig. 8 Tension damage at 1.66716 million cycles

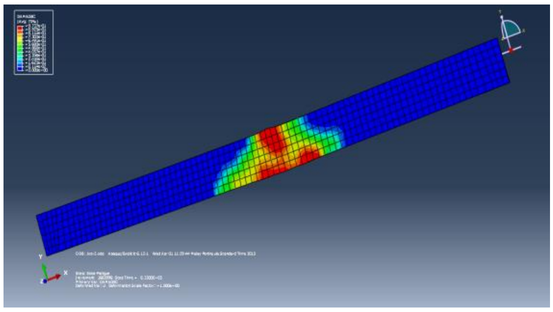
Fig. 9 Compression damage at 1.66716 million cycles

which has been achieved from the thorough studies of the representative RC beam F4. The crack pattern and displacement at failure stage are demonstrated in Fig. 6 and Fig. 7 respectively. It is obvious that the beam deflection under cyclic loading is influenced by the behavior of concrete as well as the compression and tension steel.

3.4.2 Failure modes

Fig. 8 and Fig. 9 present the failure modes of representative beams as detected from the non-linear FE analysis for the cyclically loaded RC beams. It is noticeable that the failure modes of the beams predicted from the FE investigation resembles soundly with the expected outcomes. The beam specimen F4 has been found to be failed because of concrete crushing subsequently the creation of flexural cracks in the constant moment region.

3.5 Effect of increasing loading in fatigue behavior

3.5.1 Deflection accumulation

The damage accumulation of the selected beams has been assessed in terms of the accumulation of deflection at the upper load limit. It is noteworthy that only the behavior at the upper load limit is investigated as it is more concern of designers and engineers. Nevertheless, more insight is referred into the behavior at the lower load limit. The Fig. 10 represents the alteration of mid-span deflection with the increase in the number of cycles.

The maximum deflection increases as the number of cycles increase. There are three stages of deflection behavior for the RC beams under cyclic loads. The deflection increases during the first 10% of the beam fatigue life. The deflection escalates by 52 and 88% at the end of fatigue loading compared to the first cycle case for beams F6 and F8 than F4 respectively. This shows clearly the loading effect as these increment of deflection are for 10% and 20% increase of upper load respectively. Then there are constant deflections in the second phase and shows an increase just before failure. The deflections at failure stage for 10~60% and 10~70% load range are 22% and 44% greater than the deflection in case of 10~40% load ranged failure stage. Hence, for beams fatigued at increasing stress range, the beams resulted in increased deflection at the end of fatigue loading but at the same time resulted in lowering the percentage deflection increase.

3.5.2 Strain evolution

An overall rise of concrete compressive strains at the early loading stage has been observed. This is possibly because of concrete softening and creep for cyclic loading. The variation of mid-span strain distribution has been presented in Fig. 11 at different number of cycles at the upper fatigue load limit for beams F4, F6 and F8. Almost a linear strain distribution is achieved during the first cycle for all the sample beams. The strain values increase rapidly once the beams have been fatigued. For beam F6 the strain increases by 24% while for case F8, the strain enhances by 35% at the end of initial cycle. Strains at the top level of concrete rise speedily within the initial 200000 cycles. After

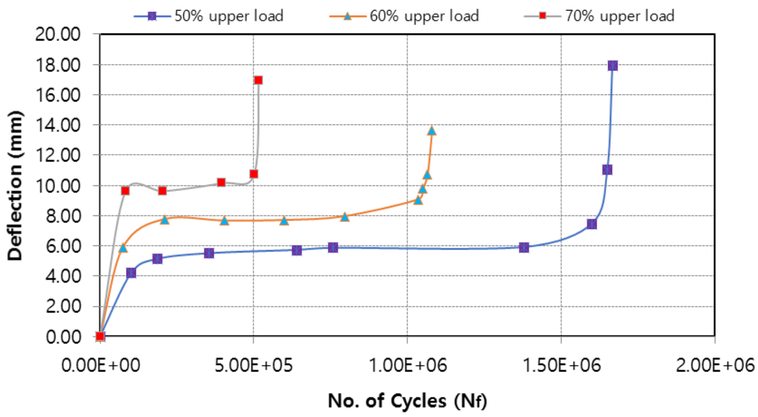

Fig. 10 Variation of mid-span deflection for loading intensity

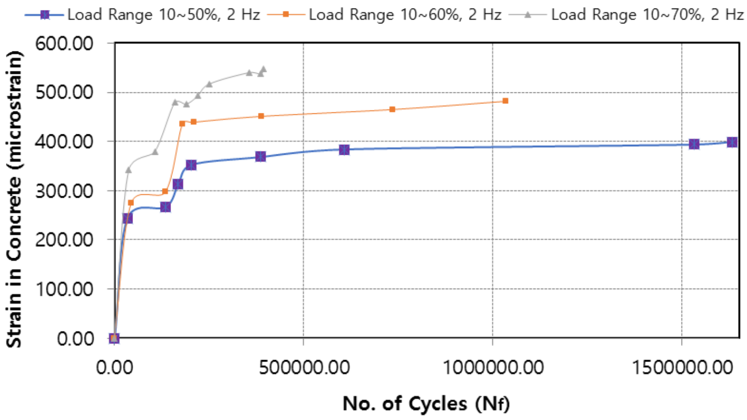

Fig. 11 Variation of mid-span strain in concrete

that there is a stabilized increase until the end of fatigue loading. At this second phase after initial cycle, the strain distribution almost maintains its linearity during the fatigue loading for the RC beam specimens. However, the rate of strain increase is higher for the higher load cases as the occurrence of damage come faster.

4. Conclusions

Following are the major findings made from the study:

√ The behavior of numerical beam shows good agreement with the experimental beam. Hence, the present computer aided model can be used as an expedient contrivance to predict the ultimate load of RC beams.

√ The damage accumulation signified in augmented deflection rises rapidly during the initial fatigue loading followed by a stabilized continuous increasing trend. This controlled fatigue damage evolution at service fatigue load limits makes the FE model an efficient tool in predicting fatigue behavior.

√ A gradual decrease in fatigue life is seen from the S-N curve for higher loading. Developed S-N curve can be representative for prior prediction of fatigue behavior under any loading case on the RC beam.

√ The beam specimens fail owing to concrete crushing after the creation of flexural cracks in the constant moment region. Reasonably the flexural failures in higher load ranges occur gradually in lower life cycles of loading due to the load intensity. All cracks in the beam models are appeared gradually during 10000 cycles and has a tendency to upsurge in height and width in the succeeding loading cycles.

√ Maximum deflection in the RC beams increases as the load intensity increases. At the end of initial cycle (first phase), deflection increases by 52 and 88% for beams F6 and F8 than F4 respectively. Thereafter, deflections remain constant in the second phase, followed by a growth just before failure. However, at the end of fatigue loading, the rate of deflection increases for higher load decrement.

√ A general rise of peak concrete compressive strains in early loading might be for concrete softening and creep for higher cyclic loading. Strains increase rapidly within 200000 cycles showing 24% and 35% increase for 60% and 70% upper load respectively. After, the strain distribution almost maintains its linearity. Yet, the rate of strain increase upsurges in the higher load cases for faster damage occurrence.

Acknowledgement

The author thankfully acknowledges the assistance of Prof. Ir. Dr. Mohd Zamin Jumaat and Dr. Mahfuz ud Darain of University of Malaya, Malaysia as well as the Deanship of Scientific Research (DSR) project 2017-212-Eng, Imam Abdulrahman Bin Faisal University (IAU) for effectual accomplishment of the research.

References

A615M-14, A.A. (2014), Standard Specification for Deformed and Plain Carbon-Steel Bars for Concrete Reinforcement.

ACI. (1992), Considerations for design of concrete structures subjected to fatigue loading. *ACI Committee 215R-92*(Detroit).

Al-Rousan, R. and Issa, M. (2011), "Fatigue performance of reinforced concrete beams strengthened with CFRP sheets", *Constr. Build. Mater.*, **25**(8), 3520-3529. https://doi.org/10.1016/j.conbuildmat.2011.03.045.

Aslani, F. and Jowkarmeimandi, R. (2012), "Stress-strain model for concrete under cyclic loading", *Mag. Concrete Res.*, **64**(8), 673-685. http://dx.doi.org/10.1680/macr.11.00120.

ASTM. (2014), "Standard Test Method for Compressive Strength of Cylindrical Concrete Specimens ASTM C39/C39M-14", American Society for Testing and Materials (ASTM) International, USA.

Badawi, M. and Soudki, K. (2009), "Fatigue behavior of RC beams strengthened with NSM CFRP rods", *J. Compos. Constr.*, **13**(5), 415-421. https://doi.org/10.1061/(ASCE)1090-0268(2009)13:5(415).

Barros, J.A., Baghi, H., Dias, S.J. and Ventura-Gouveia, A. (2013), "A FEM-based model to predict the behaviour of RC beams shear strengthened according to the NSM technique", *Eng. Struct.*, **56**, 1192-1206. https://doi.org/10.1016/j.engstruct.2013.06.034.

Committee, A. (2011), Building Code Requirements for Structural Concrete (318-11) and Commentary-(318R-11), Detroit Mich. Am. Concr. Inst.

Desayi, P. and Krishnan, S. (1964), "Equation for the stress-strain curve of concrete", *ACI J. Proc.*, **61**(3), 345-350.

EN, B. (2009), 12390-3: 2009 Testing Hardened Concrete. Making and Curing Specimens for Strength Tests, ISBN, 940137696.

EN, B. (2009), 12390-5:2009, Flexural Strength of Test Specimens, Testing Hardened Concrete, 1-14.

Hawileh, R.A. (2012), "Nonlinear finite element modeling of RC beams strengthened with NSM FRP rods", *Constr. Build. Mater.*, **27**(1), 461-471. https://doi.org/10.1016/j.conbuildmat.2011.07.018.

Helagson, T. and Hanson, J.M. (1974), "Investigation of design factors affecting fatigue strength of reinforcing bars-statistical analysis", *ACI Spec. Publ.*, **41**, 107-138.

Hibbitt, K. (2007), ABAQUS Version 6. 7: Theory Manual, Users' Manual, Verification Manual and Example Problems Manual: Hibbitt, Karlson and Sorenson Inc.

Hu, H.T., Lin, F.M. and Jan, Y.Y. (2004), "Nonlinear finite element analysis of reinforced concrete beams strengthened by fiber-reinforced plastics", *Compos. Struct.*, **63**(3), 271-281. https://doi.org/10.1016/S0263-8223(03)00174-0.

Hu, H.T. and Schnobrich, W.C. (1989), "Constitutive modeling of concrete by using nonassociated plasticity", *J. Mater. Civil Eng.*, **1**(4), 199-216. https://doi.org/10.1061/(ASCE)0899-1561(1989)1:4(199).

Huda, M.N., Jumat, M.Z.B., Islam, A.B.M.S., Darain, K.M., Obaydullah, M. and Hosen, M.A. (2017), "Palm oil industry's bi-products as coarse aggregate in structural lightweight concrete", *Comput. Concrete*, **19**(5), 515-526. https://doi.org/10.12989/cac.2017.19.5.515.

Islam, A.B.M.S., Hussain, R.R., Jumaat, M.Z. and Darain, K.M. (2014), "Implication of rubber-steel bearing nonlinear models on soft storey structures", *Comput. Concrete*, **13**(5), 603-619. http://dx.doi.org/10.12989/cac.2014.13.5.603.

Islam, A.B.M.S., Jumaat, M.Z., Hussain, R.R., Hosen, M.A. and Huda, M.N. (2015), "Incorporation preference for rubber-steel bearing isolation in retrofitting existing multi storied building", *Comput. Concrete*, **16**(4), 503-529. http://dx.doi.org/10.12989/cac.2015.16.4.503.

Kupfer, H., Hilsdorf, H. K. and Rusch, H. (1969), "Behavior of concrete under biaxial stresses", *ACI J. Proc.*, **66**(8), 656-666.

Maekawa, K., Okamura, H. and Pimanmas, A. (2003), *Non-linear Mechanics of Reinforced Concrete*, CRC Press.

Moss, D.S. (1982). Bending Fatigue of High-yield Reinforcing Bars in Concrete, TRRL Supplementary Rep. No. 748.

Nilson, A.H. (1982), "State-of-the-art report on finite element analysis of reinforced concrete", American Society of Civil Engineers: Task Committee on Finite Element Analysis of Reinforced Concrete Structures of the Structural Division Committee on Concrete and Masonry Structures, ASCE, New York, NY.

Omran, H.Y. and El-Hacha, R. (2012), "Nonlinear 3D finite element modeling of RC beams strengthened with prestressed NSM-CFRP strips", *Constr. Build. Mater.*, **31**, 74-85. https://doi.org/10.1016/j.conbuildmat.2011.12.054.

Rahman, M.M., Jumaat, M.Z. and Islam, A.B.M.S. (2017). Weight minimum design of concrete beam strengthened with glass fiber reinforced polymer bar using genetic algorithm", *Comput. Concrete*, **19**(2), 127-131. https://doi.org/10.12989/cac.2017.19.2.127.

Sarkani, Michaelov, G., Kihl, D.P. and Bonanni, D.L. (2001), "Comparative study of nonlinear damage accumulation models in stochastic fatigue of FRP laminates", *J. Struct. Eng.*, **127**(3), 314-322. https://doi.org/10.1061/(ASCE)0733-9445(2001)127:3(314).

Sasaki, K.K., Paret, T., Araiza, J.C. and Hals, P. (2010), "Failure of concrete T-beam and box-girder highway bridges subjected to cyclic loading from traffic", *Eng. Struct.*, **32**(7), 1838-1845. https://doi.org/10.1016/j.engstruct.2010.01.006.

Sohel, K.M.A., Al-Jabri, K., Zhang, M.H. and Liew, J.Y.R. (2018), "Flexural fatigue behavior of ultra-lightweight cement composite and high strength lightweight aggregate concrete", *Constr. Build. Mater.*, **173**, 90-100. https://doi.org/10.1016/j.conbuildmat.2018.03.276.

Suidan, M. and Schnobrich, W.C. (1973), "Finite element analysis of reinforced concrete", *J. Struct. Div.*, **99**(10), 2109-2122.

Zhang, S. and Teng, J. (2014), "Finite element analysis of end cover separation in RC beams strengthened in flexure with FRP", *Eng. Struct.*, **75**, 550-560. https://doi.org/10.1016/j.engstruct.2014.06.031.

HK